

## REGENERATIVE ENDODONTICS

# Effect of 3-dimensional Collagen Fibrous Scaffolds with Different Pore Sizes on Pulp Regeneration

Qianli Zhang, MD,<sup>\*†</sup>  
Chongyang Yuan, MD,<sup>\* Li Liu,  
PhD,<sup>‡</sup> Shipeng Wen, PhD,<sup>‡</sup> and  
Xiaoyan Wang, PhD<sup>\*</sup></sup>

## ABSTRACT

**Introduction:** In this study, we generated a 3-dimensional (3D) collagen fibrous scaffold for potential pulp regeneration and investigated the influence of various pore sizes of these scaffolds on proliferation, odontoblastic differentiation of human dental pulp cells (hDPCs), and subsequent tissue formation during pulp regeneration. **Methods:** Electrospinning followed by freeze-drying was used to fabricate 3D fibrous collagen scaffolds. hDPCs were cultured on these scaffolds. Cell growth was detected by a Cell Counting Kit-8 assay and observed via scanning electron microscopy. Odontogenic genes and protein expression were analyzed by real-time reverse transcription polymerase chain reaction and immunofluorescence staining. The formation of mineralized nodules was tested by von Kossa staining, scanning electron microscopy, and energy-dispersive X-ray microanalysis. Subcutaneous transplantation of the seeded scaffold/tooth fragments into nude mice was performed to observe tissue formation for pulp regeneration. **Results:** Collagen 3D fibrous scaffolds with 3 distinct mean pore sizes (approximately 20  $\mu\text{m}$ , 65  $\mu\text{m}$ , and 145  $\mu\text{m}$ ) were fabricated, which showed good biocompatibility and bioactivity. Scaffolds with larger mean pore sizes of 65 and 145  $\mu\text{m}$  improved hDPC ingrowth and proliferation, with the 65- $\mu\text{m}$  scaffold group presenting the highest level of odontogenic gene expression (*DSPP* and *DMP-1*), protein expression (*DMP-1*), mineralized area ratio, and vascular pulplike tissue formation after 6 weeks of subcutaneous implantation. **Conclusions:** The pore size of collagen 3D fibrous scaffolds significantly affected cell adhesion, proliferation, odontoblastic differentiation, and tissue rehabilitation. Scaffolds with a mean pore size of 65  $\mu\text{m}$  presented superior results and could be an alternative for pulp regeneration. (*J Endod* 2022; ■:1–9.)

## KEY WORDS

3-dimensional fibrous scaffold; collagen fiber; pore size; pulp regeneration

Dental pulp infections and necrosis are common oral diseases<sup>1</sup>. Conventional endodontic treatment results in devitalized and weakened teeth<sup>2,3</sup>. Tissue engineering technology has been considered a potential approach to achieve pulp regeneration for replacing or repairing impaired pulp tissues. The basic strategy usually involves stem cells, scaffolds, and bioactive molecules. Scaffolds play a vital role in this process, serving as a 3-dimensional (3D) tissue template, and support cell attachment, proliferation, differentiation, and neotissue genesis.

An advanced scaffold can mimic certain advantageous features of the natural extracellular matrix (ECM)<sup>4</sup>. Collagen type I is the main component of the organic substances in the pulp ECM. The collagen matrix reportedly promotes proliferation, odontogenic differentiation, and mineralization and has been used as a scaffold in tooth tissue engineering<sup>5,6</sup>. Moreover, collagen type I persists in natural ECM in the form of nanofibers. Much of the previous efforts have demonstrated that the fibrous structure of scaffolds can promote human dental pulp stem cell (hDPSC) attachment, proliferation, and odontogenic differentiation<sup>7–9</sup>. Electrospinning is considered an efficient approach for creating fibrous collagen matrices. Electrospun collagen fibrous scaffolds have high porosity and a high surface-to-volume ratio and thus are beneficial for cell growth<sup>10,11</sup>. In recent years, electrospun collagen fibrous scaffolds have been created for tissue engineering<sup>12–15</sup> but have rarely been applied for pulp regeneration.

## SIGNIFICANCE

Collagen fibrous scaffolds with a mean pore size of 65  $\mu\text{m}$  seeded with hDPCs presented optimal cell adhesion, proliferation, odontoblastic differentiation *in vitro*, and vascularized pulplike tissue formation *in vivo*, suggesting its potential application as a scaffold for pulp regeneration.

From the <sup>\*</sup>Department of Cariology and Endodontology, National Engineering Laboratory for Digital and Material Technology, Peking Key Laboratory of Digital Stomatology, and <sup>†</sup>4th Dental Department, Peking University School and Hospital of Stomatology; and <sup>‡</sup>Beijing Engineering Research Centre of Advanced Elastomers, Beijing University of Chemical Technology, Beijing, China

Address requests for reprints to Dr Shipeng Wen, Beijing Engineering Research Centre of Advanced Elastomers, Beijing University of Chemical Technology, Beijing 100029, China. Dr Xiaoyan Wang, Department of Cariology and Endodontology, National Engineering Laboratory for Digital and Material Technology, Peking Key Laboratory of Digital Stomatology, Peking University School and Hospital of Stomatology, Beijing 100081, China. E-mail addresses: [wensp@mail.buct.edu.cn](mailto:wensp@mail.buct.edu.cn) or [wangxiaoyan@pkuss.bjmu.edu.cn](mailto:wangxiaoyan@pkuss.bjmu.edu.cn) 0099-2399/\$ - see front matter

Copyright © 2022 American Association of Endodontists.

<https://doi.org/10.1016/j.joen.2022.10.007>

The microarchitectures of scaffolds have also been shown to significantly modulate cell-matrix interaction<sup>16</sup>. The mean pore size of the scaffold can especially affect cell behavior both *in vitro* and *in vivo*. Scaffolds with large pores reportedly promote cell migration and material transport; however, their mechanical strength and durability are typically sacrificed<sup>17,18</sup>. Although scaffolds with small pores provide a high surface area for cell adhesion<sup>19</sup>, the small pore size limits cell infiltration<sup>20–22</sup>. For different cells, proper pore sizes are distinct. Compared with scaffolds with larger pore sizes of 75–200  $\mu\text{m}$ , those with relatively smaller pore sizes of 10–75  $\mu\text{m}$  may be more favorable for the regeneration of connective tissue<sup>23</sup>. Dental pulp is a special type of connective tissue. Therefore, scaffolds with relatively small pore sizes are presumably beneficial for pulp regeneration. However, only a few recent studies have explored the effect of scaffold pore size on pulp regeneration. Silk scaffolds with different pore sizes have been previously explored. A 500- $\mu\text{m}$  pore size scaffold presented more robust osteodentinlike mineralized tissue formation than a 250- $\mu\text{m}$  pore size scaffold<sup>24</sup> and similar soft and hard tissue regeneration to a 1,000- $\mu\text{m}$  pore size scaffold *in vivo*<sup>25</sup>. The pore sizes of the scaffolds were large, which may negate their effect on pulp regeneration. Another study found that a poly lactic-co-glycolic acid scaffold with an extremely small pore size (<5  $\mu\text{m}$ ) could promote dentinogenic differentiation of hDPCs with significantly limited cell penetration compared with scaffolds with larger pore sizes (45–10  $\mu\text{m}$  and 10–5  $\mu\text{m}$ )<sup>26</sup>. However, the pore sizes selected in this study were too small to permit highly vascularized tissue formation<sup>27</sup>.

In this study, we used electrospinning combined with freeze-drying to fabricate 3D collagen fibrous scaffolds, and 3 graded freezing temperatures that were readily available in the laboratory were used to generate scaffolds with 3 distinct mean pore sizes (ie, 20, 65, and 145  $\mu\text{m}$ ). The key goal of this study was to generate a 3D collagen fibrous scaffold for potential pulp regeneration and to investigate the influence of various mean pore sizes of these scaffolds on *in vitro* proliferation, odontoblastic differentiation, and *in vivo* pulp regeneration (Fig. 1).

## MATERIALS AND METHODS

### Preparation and Characterization of 3D Collagen Ultrafine Fibrous Scaffolds

Collagen powder (Sannie, Tianjin, China) was dissolved in tetrafluoroethylene (Aladdin, Shanghai, China) at 6% (w/v) and then

electrospun into collagen ultrafine fibrous mats. After the mats were pre-cross-linked for 4 hours with 1-(3-Dimethylaminopropyl)-3-ethylcarbodiimide Hydrochloride/N-hydroxysuccinimide (TCI, Shanghai, China) solution, they were used to fabricate 3D collagen ultrafine fibrous scaffolds with different mean pore sizes, following the method of a previous study<sup>28</sup>. Briefly, pre-cross-linked mats were ground to short ultrafine fibers and/or tiny pieces of collagen. Subsequently, they were uniformly dispersed in 6.0 mL deionized water containing 2.5% (w/v) ethanol at 1 mg/mL. The resulting suspension was stored in 48-well plates; frozen at  $-196^{\circ}\text{C}$ ,  $-80^{\circ}\text{C}$ , or  $-20^{\circ}\text{C}$  for 2 hours; freeze-dried for 24 hours; and cross-linked sufficiently. The surface morphologies of the scaffolds were observed by scanning electron microscopy (SEM) (S-4800; Hitachi, Tokyo, Japan). ImageJ software (National Institutes of Health, Bethesda, MD) was used to measure pore sizes based on the scanning electron microscopic images. The detailed methodology is provided in the [Supplemental Materials and Methods](#) (available online at [www.jendodon.com](http://www.jendodon.com)).

### Cell Culture of Human Dental Pulp Cells

Human dental pulp cells were isolated from the third molars of healthy people; they were provided by Peking University Hospital of Stomatology, Haidian District, Beijing, China. Experiments were performed in compliance with the relevant laws and institutional guidelines of Peking University and approved by the Experimental Animal Welfare Ethics Section of the Peking University Biomedical Ethics Committee (PKUSSIRB-201943038). The cells were cultured in growth medium (Dulbecco's Modified Eagle's Medium; ScienCell, Carlsbad, CA) supplemented with 10% fetal bovine serum (ScienCell), 100 U/mL penicillin, and 100  $\mu\text{g}/\text{mL}$  streptomycin (ScienCell). The cells were maintained at  $37^{\circ}\text{C}$  in a 5%  $\text{CO}_2$  and 95% humidity atmosphere. The medium was changed every 2 or 3 days, and hDPCs cultured between the third and sixth passages were used for subsequent experiments.

### Proliferation of hDPCs in 3D Scaffolds

The hDPCs ( $5 \times 10^4$  cells/scaffold) were seeded on the 3D scaffolds with various mean pore sizes, and cell proliferation ability was detected by the Cell Counting Kit-8 assay after 1, 3, 5, and 7 days. To observe the cell morphology and distribution on the scaffolds, SEM was performed on day 7. The detailed

methodology is provided in the [Supplemental Materials and Methods](#) (available online at [www.jendodon.com](http://www.jendodon.com)).

### Odontogenic Differentiation of hDPCs in 3D Scaffolds

The hDPCs ( $2 \times 10^5$  cells/scaffold) were seeded on the 3D scaffolds with various mean pore sizes and were cultured in odontogenic differentiation medium, Dulbecco's Modified Eagle's Medium supplemented with 10% fetal bovine serum, 100 U/mL penicillin, 100  $\mu\text{g}/\text{mL}$  streptomycin, 10 nmol/L dexamethasone (Sigma-Aldrich, St Louis, MO), 5 mmol/L  $\beta$ -glycerophosphate (Sigma-Aldrich), and 50  $\mu\text{g}/\text{L}$  ascorbic acid (Sigma-Aldrich). Gene expressions of alkaline phosphatase (ALP), dentin sialophosphoprotein (DSPP), and dentin matrix protein-1 (DMP-1) were quantified by real-time reverse transcription polymerase chain reaction at 1, 2, and 3 weeks. Protein expression of DMP-1 was observed via confocal laser scanning microscopy (SP8; Leica, Wetzlar, Germany) at 4 weeks. The formation of mineralized nodules was tested by von Kossa staining, SEM, and energy-dispersive X-ray microanalysis (EDX) at 4 weeks. The detailed methodology is provided in the [Supplemental Materials and Methods](#) (available online at [www.jendodon.com](http://www.jendodon.com)).

### In Vivo Animal Experiments

All animal experiments were performed in compliance with the relevant laws and institutional guidelines of Peking University and were approved by the Experimental Animal Welfare Ethics Section of the Peking University Biomedical Ethics Committee (approval number: PKUSSIRB-201943038). The molars of healthy people were provided by the Peking University Hospital of Stomatology. The crowns of the freshly pulled teeth were cut into fragments with a thickness of 2.5 mm, and the pulp cavities were expanded to a diameter of 3 mm. The tooth fragments were disinfected using 5.25% sodium hypochlorite and 17% EDTA. The hDPC-seeded scaffolds ( $1 \times 10^5$  cells/scaffold) were implanted into the tooth fragments and cultured for 1 week in growth medium. The seeded scaffold/tooth fragments were then implanted into subcutaneous pockets created by blunt lateral dissection in 6-week-old nude male mice. Each mouse received 2 samples. Six weeks later, all implants were retrieved and fixed in 4% paraformaldehyde, decalcified, and processed for hematoxylin-eosin staining and immunohistochemical (IHC) analysis of CD31 and DMP-1 (Abcam, Cambridge, UK). The detailed methodology is provided in the

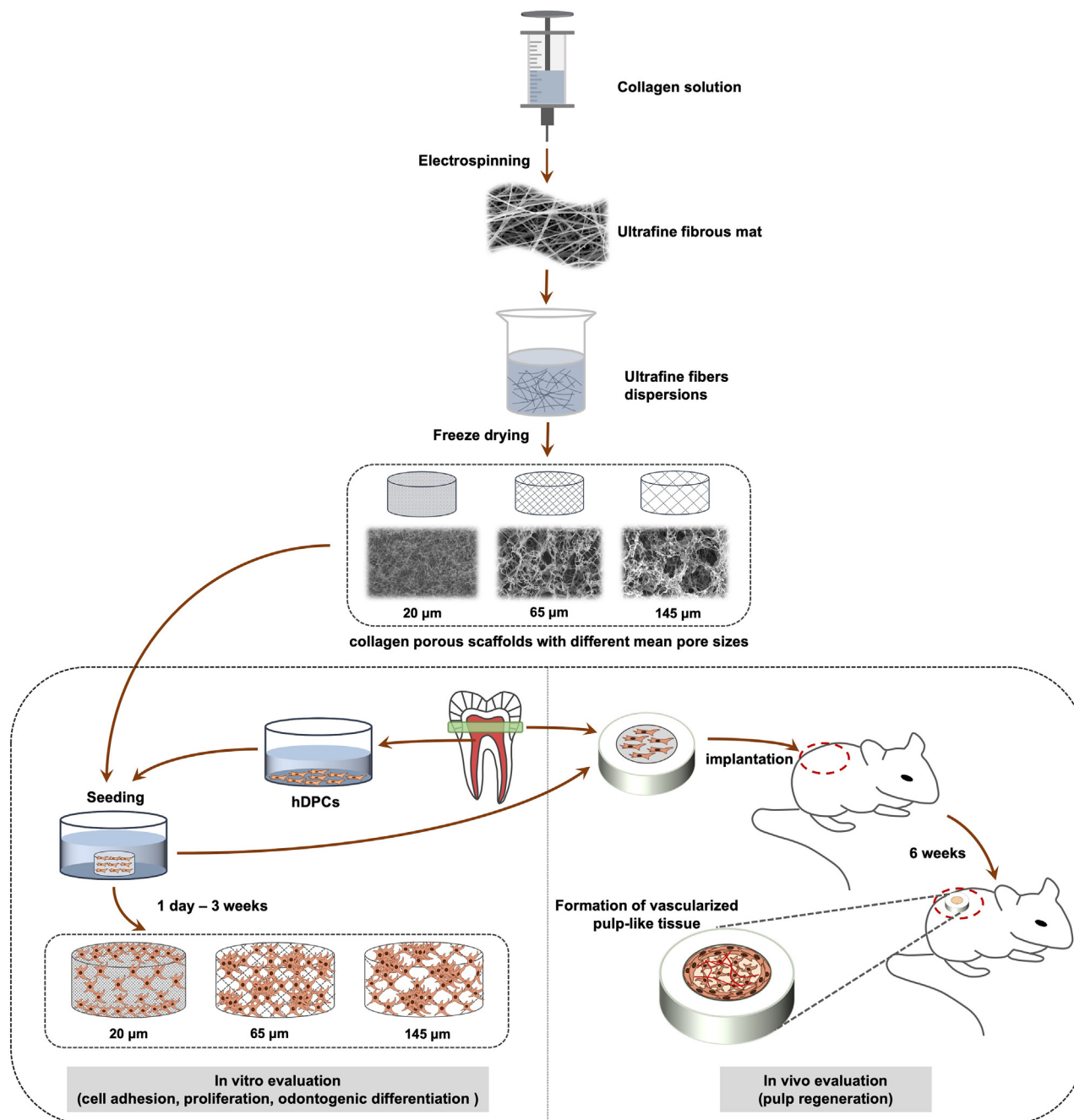


**FIGURE 1** – A schematic illustration for the preparation and evaluation of collagen fibrous scaffolds with different mean pore sizes for pulp regeneration *in vitro* and *in vivo*.

Supplemental Materials and Methods  
(available online at [www.jendodon.com](http://www.jendodon.com)).

### Statistical Analysis

All statistical data are expressed as mean  $\pm$  standard deviation. All experiments were repeated at least 3 times. Statistical significance was determined using 1-way analysis of variance. Multiple comparisons between the groups were performed using the

post hoc Tukey multiple comparison test (for 1-way analysis of variance). Statistical significance was set at  $P < .05$ .

## RESULTS

### Fabrication and Characteristics of Collagen Scaffolds

The gross appearance of these scaffolds was similar (Fig. 2A). Scanning electron microscopic observations showed the microstructures and

morphologies of the 3D collagen scaffolds (Fig. 2B–D). The different scaffolds had similar interconnected and hierarchically structured pores. The large major pores were evenly distributed and stacked, and many small holes were observed on the ultrafine walls of the large pores. The mean sizes of the major pores in the collagen scaffolds prepared at  $-196^{\circ}\text{C}$ ,  $-80^{\circ}\text{C}$ , and  $-20^{\circ}\text{C}$  were  $20 \pm 6 \mu\text{m}$  (20  $\mu\text{m}$ ),  $64 \pm 15 \mu\text{m}$  (65  $\mu\text{m}$ ), and  $144 \pm 36 \mu\text{m}$  (145  $\mu\text{m}$ ), respectively. The aperture

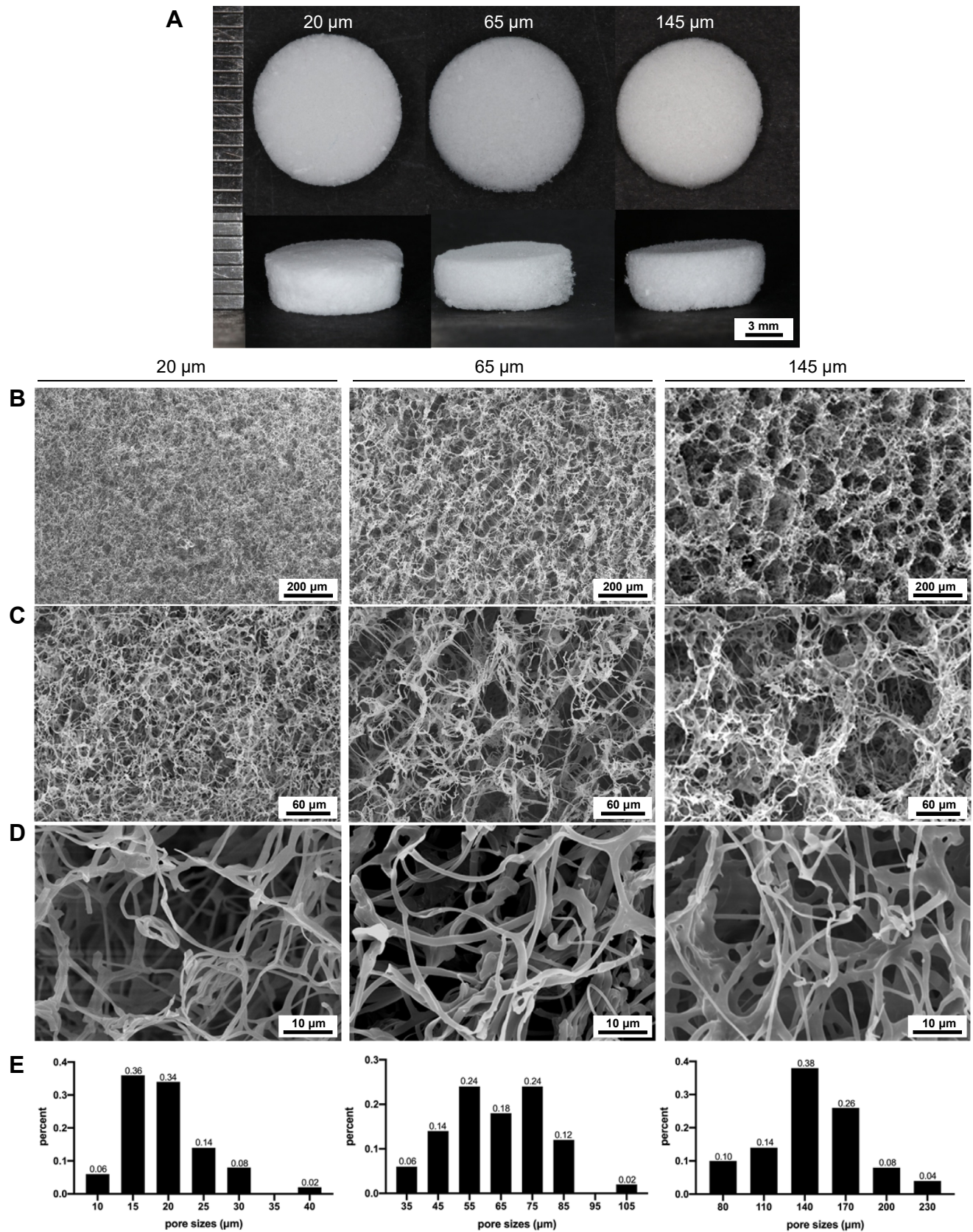


**FIGURE 2** – Gross appearances of the (A) frontal and lateral view, scanning electron microscopic photomicrographs of the cross-section for (B and C) major pores and (D) ultrafibrillar walls, and (E) aperture distribution of the 3 types of collagen porous scaffolds prepared at  $-196^{\circ}\text{C}$ ,  $-80^{\circ}\text{C}$ , and  $-20^{\circ}\text{C}$  of frozen temperature; the mean pore sizes were 20  $\mu\text{m}$ , 65  $\mu\text{m}$ , and 145  $\mu\text{m}$ , respectively. Low magnification is shown in B, medium magnification in C, and high magnification in D.

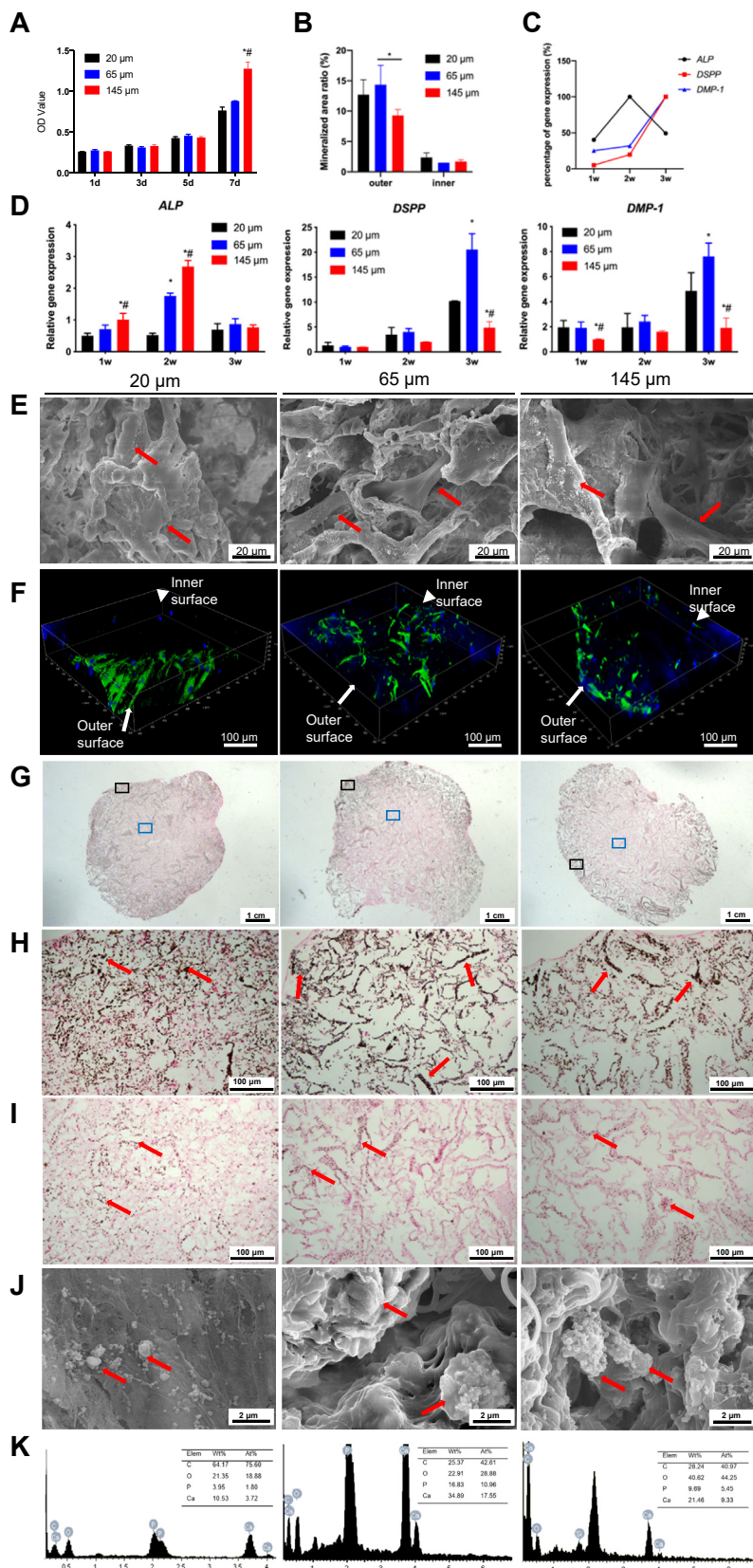


**FIGURE 3** – Proliferation and odontogenic differentiation of hDPCs cultured on scaffolds with different pore sizes. (A) CCK-8 assay. \*Compared with the 20- $\mu\text{m}$  group,  $P < .05$ . #Compared with the 65- $\mu\text{m}$  group,  $P < .05$ . (B) Quantitative measurement of the mineralized area based on the von Kossa staining results. (C) A concluding summary figure of differentiation over time. (D) Quantitative determination of messenger RNA expression of odontogenic differentiation

distributions of these 3 types of collagen scaffolds are shown in [Figure 2E](#).

### Effect of Scaffold Mean Pore Size on Proliferation and Odontogenic Differentiation of hDPCs

The Cell Counting Kit-8 assay showed that hDPCs grew well on scaffolds with different mean pore sizes and that cells on the scaffold with a 145- $\mu\text{m}$  pore size presented the highest proliferation rate at day 7 ( $P < .05$ ) ([Fig. 3A](#)). According to the scanning electron microscopic results, cells adhered well along the collagen fibers with a typical fibroblastic morphology on all types of scaffolds ([Fig. 3E](#)). Numerous cells grew into the depth of scaffolds with 145- $\mu\text{m}$  and 65- $\mu\text{m}$  pore sizes; however, cells on scaffolds with a 20- $\mu\text{m}$  pore size were primarily spread on the superficial layer of the scaffold, causing unclear individual cell morphology.

A concluding summary figure of differentiation over time is shown in [Figure 3C](#). The expression levels of *ALP* genes of hDPCs cultured on scaffolds peaked at 2 weeks and decreased by 3 weeks in 3 groups. At 2 weeks, the *ALP* expression levels increased as the pore sizes of scaffolds increased ([Fig. 3D](#)). The expression levels of *DSPP* and *DMP-1* genes of hDPCs cultured on scaffolds increased with culture time, and, at 3 weeks, they were highest on scaffolds with a 65- $\mu\text{m}$  pore size followed by those with a 20- $\mu\text{m}$  pore size; they were lowest on scaffolds with a 145- $\mu\text{m}$  pore size ([Fig. 3D](#)). According to the confocal laser scanning microscopic images ([Fig. 3F](#)), *DMP-1* expression was high throughout the outer surface but varied on the inner surface of all scaffolds. In the 65- $\mu\text{m}$  and 145- $\mu\text{m}$  pore size groups, *DMP-1* expression was detected on the inner surface of scaffolds and was evidently higher on the scaffold with a 65- $\mu\text{m}$  pore size. On scaffolds with a 20- $\mu\text{m}$  pore size, *DMP-1* expression was primarily concentrated on the outer surface. The mineralization ability of hDPCs on scaffolds was confirmed by von Kossa staining ([Fig. 3G–I](#)), SEM ([Fig. 3J](#)), and EDX ([Fig. 3K](#)). Mineral depositions were generated along the major pores of scaffolds and primarily deposited on the outer surface of all scaffolds. The mineralized area ratio was highest on the outer scaffolds with a 65- $\mu\text{m}$  pore size followed by those with a 20- $\mu\text{m}$  pore size and was lowest on the outer scaffolds with a 145- $\mu\text{m}$  pore size ([Fig. 3B](#)). The mineralized area ratio on the inner scaffolds was similar among the 3 groups ([Fig. 3B](#)).

### Effect of Scaffold Mean Pore Size on Pulp Regeneration in Vivo

[Figure 4A](#) shows the comprehensive view of tooth fragments with and without seeded

scaffolds and the tooth fragments that were fully filled with smooth soft tissues. The hematoxylin-eosin staining (Fig. 4B) results showed that in the empty tooth fragments, only a small amount of connective tissue was formed, whereas in the seeded scaffold tooth fragment groups, most of the scaffolds degraded after 6 weeks and were replaced by regenerated pulplike tissue with rich blood vessels. A layer of cells was observed lining the pulp-dentin interface in the seeded scaffold tooth fragments, which was thicker in the 65- $\mu\text{m}$  and 20- $\mu\text{m}$  pore size groups than in the 145- $\mu\text{m}$  pore size group. The cells were identified as odontoblastlike cells with positive DMP-1 staining along the dentin wall (Fig. 4C). The mean integrated optical density of DMP-1 staining in the outer scaffold near the dentin wall decreased as the pore sizes increased (Fig. 4E). Moreover, the angiogenic protein CD31 was detected (Fig. 4D), and blood vessel ingrowth was confirmed in the 3 groups; the number of blood vessels in the inner scaffolds with a 20- $\mu\text{m}$  pore size was significantly the lowest (Fig. 4F).

## DISCUSSION

The advanced microarchitecture of scaffolds, particularly the mean pore size, significantly affects cell behavior and subsequent tissue formation and is a prerequisite for successful tissue engineering<sup>29–32</sup>. However, the optimal pore size for pulp regeneration has seldom been reported and lacks a consensus opinion<sup>24,25</sup>. In this study, porous collagen scaffolds with different mean pore sizes (145, 65, and 20  $\mu\text{m}$ ) were fabricated, which demonstrated potential for pulp regeneration.

According to the results of the adhesion and proliferation of hDPCs *in vitro*, the scaffolds with the smallest mean pore size of 20  $\mu\text{m}$  had the lowest cell infiltration and cell proliferation rate compared with those with relatively larger mean pore sizes of 145 and 65  $\mu\text{m}$ . Although the scaffold with the smallest mean pore size can provide the largest area for cell adhesion, colonization, and subsequent proliferation, the latter 2 groups with larger pore sizes are more easily accessible to cells. Thus, the larger pore sizes of 145 and 65  $\mu\text{m}$  may be favorable for scaffolds for hDPC growth.

Another notable result from the study is that the mean pore sizes of scaffolds would influence odontoblastic differentiation of

hDPCs *in vitro*. The expression levels of *ALP* increase with the pore sizes of scaffolds within the pore size range in this study, which was consistent with previous studies on bone tissue engineering. *ALP* regulates organic and inorganic metabolism, acts as a plasma membrane transporter for inorganic phosphates<sup>33</sup>, and is widely used as an early marker of osteogenic differentiation. In this study, the expression levels of *ALP* peaked at 2 weeks and declined by 3 weeks<sup>21</sup>. The trends of the expression levels of *DSPP* and *DMP-1* were different from that of *ALP*. Thus, odontogenic differentiation and osteogenic differentiation have many similarities, but they are always different. The expression levels of *DSPP* and *DMP-1* were highest on scaffolds with a 65- $\mu\text{m}$  pore size followed by scaffolds with a 20- $\mu\text{m}$  pore size and were lowest on scaffolds with a 145- $\mu\text{m}$  pore size. This may be because the scaffolds with a 65- $\mu\text{m}$  pore size may provide a more proper niche to increase cell-cell interaction, providing a 3D microenvironment to promote odontoblastic differentiation. This assumption is in accordance with immunofluorescence staining and von Kossa staining results, which respectively validated the expression of proteins related to odontogenic differentiation (*DMP-1*) at the translational level and the ability to direct mineralization.

Consistent with the *in vitro* results, scaffolds with a 65- $\mu\text{m}$  pore size also displayed superior potential for pulp regeneration *in vivo* in which a high vascularity pulplike tissue was formed. Because there is no specific marker for odontoblasts to date, we used DMP-1 IHC staining and visual analysis of cell organization to determine that the cells along the dentin-pulp interface were odontoblastlike cells. DMP-1 protein expression near the dentin-pulp interface was highest on the scaffolds with a 20- $\mu\text{m}$  pore size followed by those with a 65- $\mu\text{m}$  pore size and were lowest on scaffolds with a 145- $\mu\text{m}$  pore size. The potential reason is that the scaffolds with a 65- $\mu\text{m}$  pore size may provide a more proper niche to increase the cell-cell interaction than those with a 145- $\mu\text{m}$  pore size. For scaffolds with a 20- $\mu\text{m}$  pore size, hDPCs were highly aggregated on the outer surface of the scaffold, benefiting in odontoblastic differentiation. Notably, the small mean pore size of the 20- $\mu\text{m}$  scaffold hindered blood vessel ingrowth, which is consistent with previous studies<sup>34,35</sup>.

This study is a primary exploration of the mean pore sizes of collagen scaffolds, which are seldom reported and lack consensus opinions yet might be a crucial factor for pulp regeneration. However, in this study, only 3 distinct mean pore sizes (20, 65, and 145  $\mu\text{m}$ ) were evaluated, and different material scaffolds with diverse mean pore sizes should be investigated in the future. Notably, the previous scaffolds used for such comparisons were prepared via porogen leaching methods<sup>24,25</sup> in which some of the pores are interconnected but some are isolated, and the conventional porogen is difficult to remove completely, which may harm the biocompatibility of the scaffolds. These problems were resolved in this study because the electrospun fibrous frame ensured an interconnected porous structure. During the freeze-drying process, only pure water and ethanol were used, and no impurities were introduced. Therefore, the present results provide a reliable method for the direct fabrication of biocompatible and interconnected porous scaffolds with various mean pore sizes by fine control of the freezing temperature.

This study mainly focused on investigating the influence of mean pore sizes of scaffolds on pulp regeneration, whereas many other topographic features (ie, roughness, patterns, and porosity) and stiffness also play a vital role in regulating cellular responses and deserve further exploration for pulp regeneration in the future. Because cells can respond to topographic cues down to 5 nm, many micro- and nanoscale surface topographies of scaffolds were fabricated to instruct cell behaviors<sup>36</sup>. Increased roughness and specific patterns can promote dental pulp stem cell adhesion, proliferation, and differentiation<sup>37</sup>. An appropriate porosity is also essential to control biological functions. The porosities of scaffolds in this study are theoretically similar and high<sup>38</sup>. Scaffolds with high porosities will facilitate the ingrowth of cells, allow for the circulation of nutrients and wastes, and have been proven to promote new bone regeneration<sup>36</sup>. Material elasticity can also affect the differentiation of stem cells<sup>39</sup>, and dental pulp stem cells on a soft matrix tended to differentiate into pulplike tissue rather than mineralized tissue<sup>40</sup>. Considering natural collagen materials and a high porosity of scaffolds with weak mechanical strength, we suppose the difference of stiffness among the scaffolds in this study might have limited effects on cell behaviors.

Furthermore, this study analyzed the effect of the mean pore size of scaffolds on pulp regeneration, and how the hDPCs interacted with scaffolds in the microenvironment should be further investigated. Moreover, only subcutaneous

marker genes (*ALP*, *DSPP*, and *DMP-1*). \*Compared with the 20- $\mu\text{m}$  group,  $P < .05$ . #Compared with the 65- $\mu\text{m}$  group,  $P < .05$ . (E) Morphologies of hDPCs observed by SEM. (F) DMP-1 protein expression for hDPCs cultured for 4 weeks by immunofluorescence staining. (G–K) The ability of mineralization of hDPCs. (G–I) Von Kossa staining; H and I are the magnification images of the black and blue box in G. (J) Scanning electron microscopic images. (K) EDX analysis of mineral deposition in I. The red arrows point to mineral deposition.

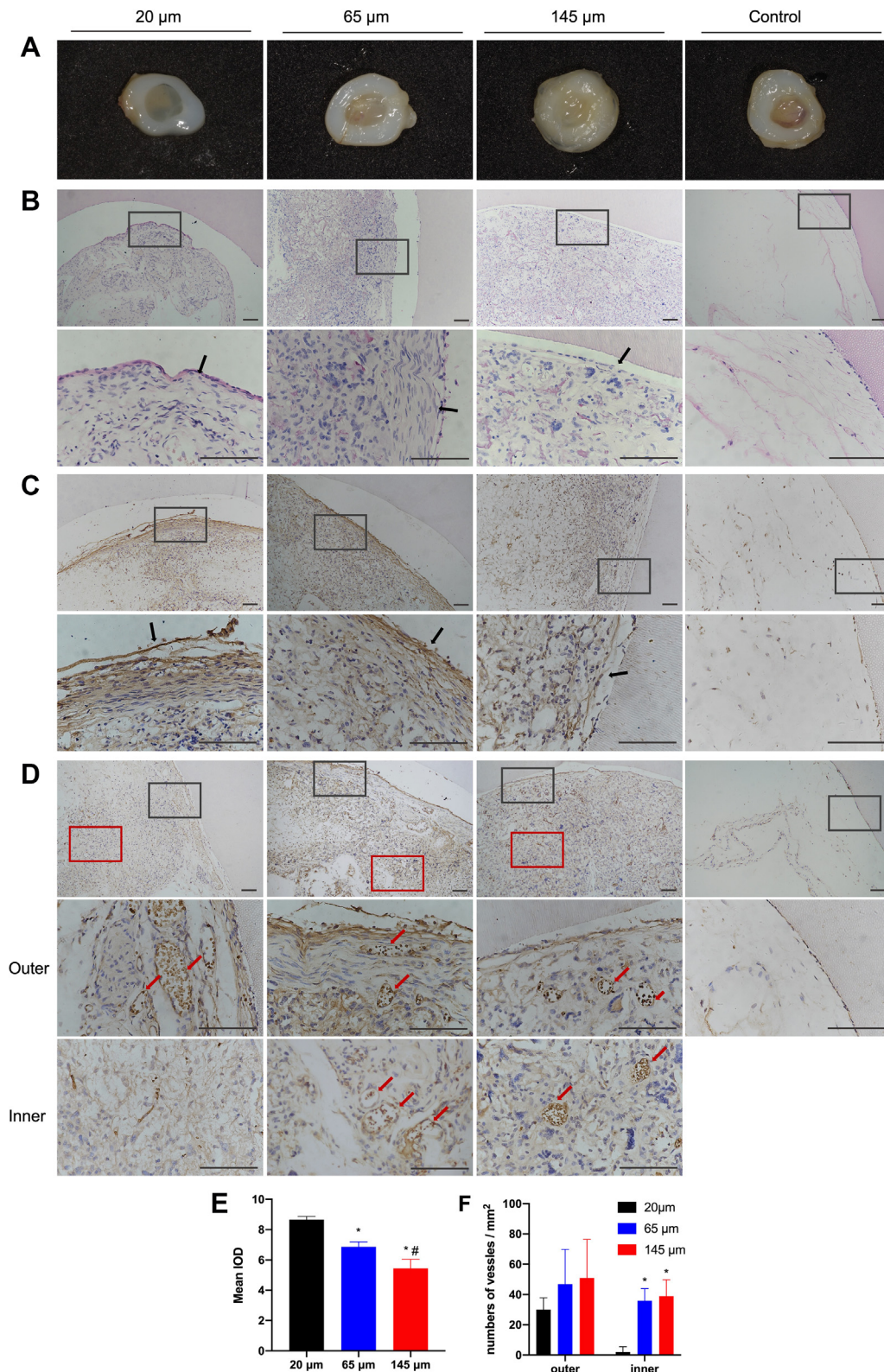


**FIGURE 4** – The (A) gross appearance and (B and C) histologic analysis of tissue regeneration in dentin slices after transplantation for 6 weeks. (B) Hematoxylin-eosin staining, (C) IHC analysis of odontogenic differentiation marker protein DMP-1, and (D) IHC analysis of angiospecific protein CD31. For each sample, images were taken at  $\times 100$  (upper row) and  $\times 400$  (upper row). Specially, to observe the distribution of blood vessel ingrowth marked by CD31, IHC analysis was taken in both the outer (black box) and the inner (red box) scaffold at high magnification. The black arrows point to layers of cells lining along the pulp-dentin interface. The red arrows point to blood vessel ingrowth. The scale bar is 100  $\mu\text{m}$ . (E) Quantitative analysis of the mean integrated optical density of DMP-1 in the outer scaffold. (F) Quantitative analysis of the number and distribution of the regenerated blood vessels. \*Compared with the 20- $\mu\text{m}$  group,  $P < .05$ . #Compared with 65- $\mu\text{m}$  group,  $P < .05$ .

experiments in nude mice for 6 weeks were used in this study, and long-term *in vivo* evaluation and an *in situ* regenerative animal model are required. In addition, the tissue formed in this study was not the typical tubular dentin tissue. Thus, further research should be done to achieve more natural dentin-pulp-like tissue, and there is still a long way to go in achieving functional pulp regeneration in clinical applications.

In conclusion, 3D collagen fibrous porous scaffolds that mimic the native ECM provided a favorable biocompatible environment for hDPCs. The mean pore size

of the fibrous porous scaffolds affected cell adhesion, proliferation, odontoblastic differentiation, and tissue rehabilitation. 3D collagen fibrous porous scaffolds with a mean pore size of 65  $\mu\text{m}$  presented optimal cell adhesion, proliferation, odontoblastic differentiation, mineralization *in vitro*, and pulp-like tissue formation *in vivo*, offering a beneficial alternative for pulp regeneration. The results improve the understanding of cell-scaffold interactions for pulp regeneration and provide valuable insights into designing future scaffolds for pulp regeneration.

## ACKNOWLEDGMENTS

Supported by the National Natural Science Foundation of China (grant no. 51503004) and PKUSSNKP (grant no. 202107).

The authors deny any conflicts of interest related to this study.

## SUPPLEMENTARY MATERIAL

Supplementary material associated with this article can be found in the online version at [www.jendodon.com](http://www.jendodon.com) (<https://doi.org/10.1016/j.joen.2022.10.007>).

## REFERENCES

1. Dye B, Thornton-Evans G, Li X, Iafolla T. Dental caries and tooth loss in adults in the United States, 2011-2012. NCHS Data Brief 2015;197:197.
2. Dotto L, Onofre RS, Bacchi A, et al. Effect of root canal irrigants on the mechanical properties of endodontically treated teeth: a scoping review. J Endod 2020;46:596-604.
3. Rippe MP, Santini MF, Bier CA, et al. Effect of root canal preparation, type of endodontic post and mechanical cycling on root fracture strength. J Appl Oral Sci 2014;22:165-73.
4. Ma PX. Biomimetic materials for tissue engineering. Adv Drug Deliv Rev 2008;60:184-98.
5. Koike T, Polan MA, Izumikawa M, et al. Induction of reparative dentin formation on exposed dental pulp by dentin phosphophoryn/collagen composite. Biomed Res Int 2014;2014:745139.
6. Kim NR, Lee DH, Chung PH, et al. Distinct differentiation properties of human dental pulp cells on collagen, gelatin, and chitosan scaffolds. Oral Surg Oral Med Oral Pathol Oral Radiol Endod 2009;108:e94-100.
7. Kuang R, Zhang Z, Jin X, et al. Nanofibrous spongy microspheres enhance odontogenic differentiation of human dental pulp stem cells. Adv Healthc Mater 2015;4:1993-2000.
8. Soares DG, Zhang Z, Mohamed F, et al. Simvastatin and nanofibrous poly(L-lactic acid) scaffolds to promote the odontogenic potential of dental pulp cells in an inflammatory environment. Acta Biomater 2018;68:190-203.
9. Zhang QL, Dong CY, Liu L, et al. [Effects of electrospun collagen nanofibrous matrix on the biological behavior of human dental pulp cells]. Beijing Da Xue Xue Bao Yi Xue Ban 2019;51:28-34.
10. Wang X, Ding B, Li B. Biomimetic electrospun nanofibrous structures for tissue engineering. Mater Today (Kidlington) 2013;16:229-41.
11. Cui W, Zhou Y, Chang J. Electrospun nanofibrous materials for tissue engineering and drug delivery. Sci Technol Adv Mater 2010;11:014108.
12. Dhand C, Ong ST, Dwivedi N, et al. Bio-inspired *in situ* crosslinking and mineralization of electrospun collagen scaffolds for bone tissue engineering. Biomaterials 2016;104:323-38.
13. Zhang S, Chen L, Jiang Y, et al. Bi-layer collagen/microporous electrospun nanofiber scaffold improves the osteochondral regeneration. Acta Biomater 2013;9:7236-47.
14. Estévez M, Montalbano G, Gallo-Cordova A, et al. Incorporation of superparamagnetic iron oxide nanoparticles into collagen formulation for 3D electrospun scaffolds. Nanomaterials (Basel) 2022;12:181.
15. Blackstone BN, Malara MM, Baumann ME, et al. Fractional CO(2) laser micropatterning of cell-seeded electrospun collagen scaffolds enables rete ridge formation in 3D engineered skin. Acta Biomater 2020;102:287-97.
16. Chen W, Shao Y, Li X, et al. Nanotopographical surfaces for stem cell fate control: engineering mechanobiology from the bottom. Nano Today 2014;9:759-84.

17. Odelius K, Höglund A, Kumar S, et al. Porosity and pore size regulate the degradation product profile of polylactide. *Biomacromolecules* 2011;12:1250–8.
18. Zhang Y, Zhang M. Three-dimensional macroporous calcium phosphate bioceramics with nested chitosan sponges for load-bearing bone implants. *J Biomed Mater Res* 2002;61:1–8.
19. Yuan H, Kurashina K, de Bruijn JD, et al. A preliminary study on osteoinduction of two kinds of calcium phosphate ceramics. *Biomaterials* 1999;20:1799–806.
20. Ekaputra AK, Prestwich GD, Cool SM, et al. Combining electrospun scaffolds with electrosprayed hydrogels leads to three-dimensional cellularization of hybrid constructs. *Biomacromolecules* 2008;9:2097–103.
21. Karageorgiou V, Kaplan D. Porosity of 3D biomaterial scaffolds and osteogenesis. *Biomaterials* 2005;26:5474–91.
22. Soliman S, Sant S, Nichol JW, et al. Controlling the porosity of fibrous scaffolds by modulating the fiber diameter and packing density. *J Biomed Mater Res A* 2011;96:566–74.
23. Hulbert SF, Young FA, Mathews RS, et al. Potential of ceramic materials as permanently implantable skeletal prostheses. *J Biomed Mater Res* 1970;4:433–56.
24. Xu WP, Zhang W, Asrican R, et al. Accurately shaped tooth bud cell-derived mineralized tissue formation on silk scaffolds. *Tissue Eng Part A* 2008;14:549–57.
25. Zhang W, Ahluwalia IP, Literman R, et al. Human dental pulp progenitor cell behavior on aqueous and hexafluoroisopropanol based silk scaffolds. *J Biomed Mater Res A* 2011;97:414–22.
26. Gangolli RA, Devlin SM, Gerstenhaber JA, et al. A bilayered poly (lactic-co-glycolic acid) scaffold provides differential cues for the differentiation of dental pulp stem cells. *Tissue Eng Part A* 2019;25:224–33.
27. Madden LR, Mortisen DJ, Sussman EM, et al. Proangiogenic scaffolds as functional templates for cardiac tissue engineering. *Proc Natl Acad Sci U S A* 2010;107:15211–6.
28. Xu T, Miszuk JM, Zhao Y, et al. Electrospun polycaprolactone 3D nanofibrous scaffold with interconnected and hierarchically structured pores for bone tissue engineering. *Adv Healthc Mater* 2015;4:2238–46.
29. Chen R, Ma H, Zhang L, et al. Precision-porous templated scaffolds of varying pore size drive dendritic cell activation. *Biotechnol Bioeng* 2018;115:1086–95.
30. Conoscenti G, Schneider T, Stoelzel K, et al. PLLA scaffolds produced by thermally induced phase separation (TIPS) allow human chondrocyte growth and extracellular matrix formation dependent on pore size. *Mater Sci Eng C Mater Biol Appl* 2017;80:449–59.
31. Zhang ZZ, Jiang D, Ding JX, et al. Role of scaffold mean pore size in meniscus regeneration. *Acta Biomater* 2016;43:314–26.
32. Di Luca A, Szlazak K, Lorenzo-Moldero I, et al. Influencing chondrogenic differentiation of human mesenchymal stromal cells in scaffolds displaying a structural gradient in pore size. *Acta Biomater* 2016;36:210–9.
33. Liu Q, Cen L, Yin S, et al. A comparative study of proliferation and osteogenic differentiation of adipose-derived stem cells on akermanite and beta-TCP ceramics. *Biomaterials* 2008;29:4792–9.
34. Hong JK, Bang JY, Xu G, et al. Thickness-controllable electrospun fibers promote tubular structure formation by endothelial progenitor cells. *Int J Nanomedicine* 2015;10:1189–200.
35. Blakeney BA, Tambralli A, Anderson JM, et al. Cell infiltration and growth in a low density, uncompressed three-dimensional electrospun nanofibrous scaffold. *Biomaterials* 2011;32:1583–90.
36. Cun X, Hosta-Rigau L. Topography: a biophysical approach to direct the fate of mesenchymal stem cells in tissue engineering applications. *Nanomaterials (Basel)* 2020;10:2070.
37. Diana R, Ardhani R, Kristanti Y, et al. Dental pulp stem cells response on the nanotopography of scaffold to regenerate dentin-pulp complex tissue. *Regen Ther* 2020;15:243–50.
38. Yao Q, Cosme JG, Xu T, et al. Three dimensional electrospun PCL/PLA blend nanofibrous scaffolds with significantly improved stem cells osteogenic differentiation and cranial bone formation. *Biomaterials* 2017;115:115–27.
39. Jiang S, Lyu C, Zhao P, et al. Cryoprotectant enables structural control of porous scaffolds for exploration of cellular mechano-responsiveness in 3D. *Nat Commun* 2019;10:3491.
40. Qu T, Jing J, Ren Y, et al. Complete pulpodentin complex regeneration by modulating the stiffness of biomimetic matrix. *Acta Biomater* 2015;16:60–70.